

Fig. 1. (a) Geological map of the Altai region in Mongolia and China, showing various geological units, faults, and national borders. (b) Detailed geological map of the Altai region, showing various geological units, faults, and national borders. The map includes an inset map (a) showing the regional context with the Siberian Craton, Gobi Desert, and North China Craton. The main map (b) shows the Altai Mountains, Buerjin, and Habaha regions. Geological units are color-coded and patterned according to the legend, including Carboniferous volcanics, Devonian volcanics, Silurian volcanics, Proterozoic-Ordovician schists, Cambrian-Ordovician volcanics, Proterozoic-Ordovician gneiss, Sinian-Cambrian metasediments, Devonian granitic, Ultramafic-mafic, Kuerti bimodal, and Faults. National borders are indicated by dashed lines. Coordinates 48°N, 90°E, and 86°E are marked.

... (1) ... (2) ...

2. R a , a a

... (1) ... (2) ... (3) ... (4) ... (5) ...

... (1) ... (2) ... (3) ... (4) ... (5) ...

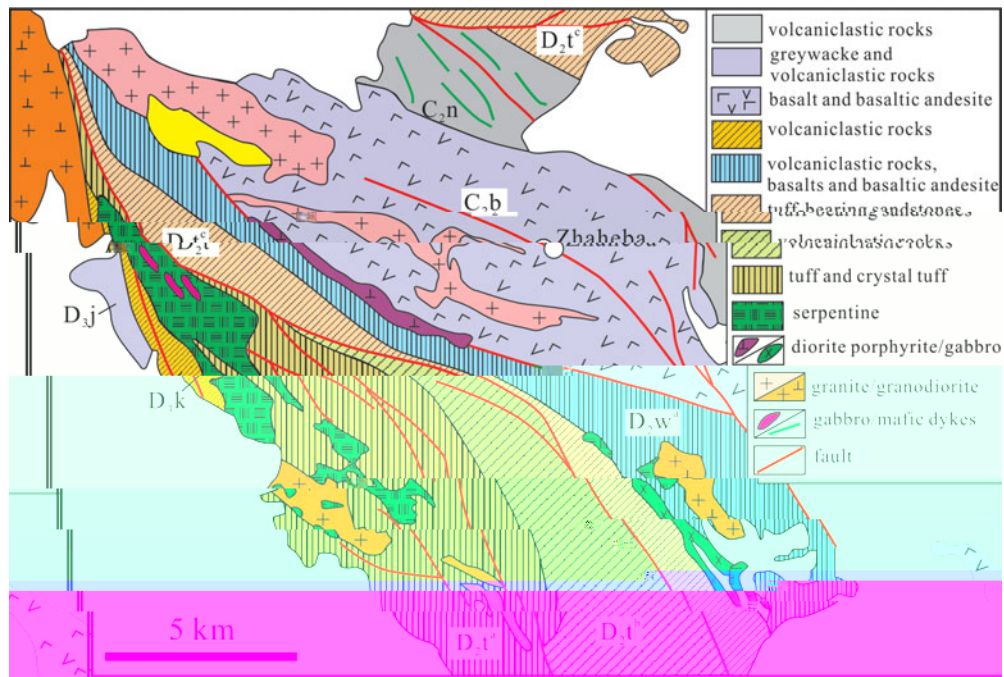


Figure 2. Geological map of the Zhaheba ophiolite (see text for details) (after Wang, et al., 2000, 2001 and 2003).

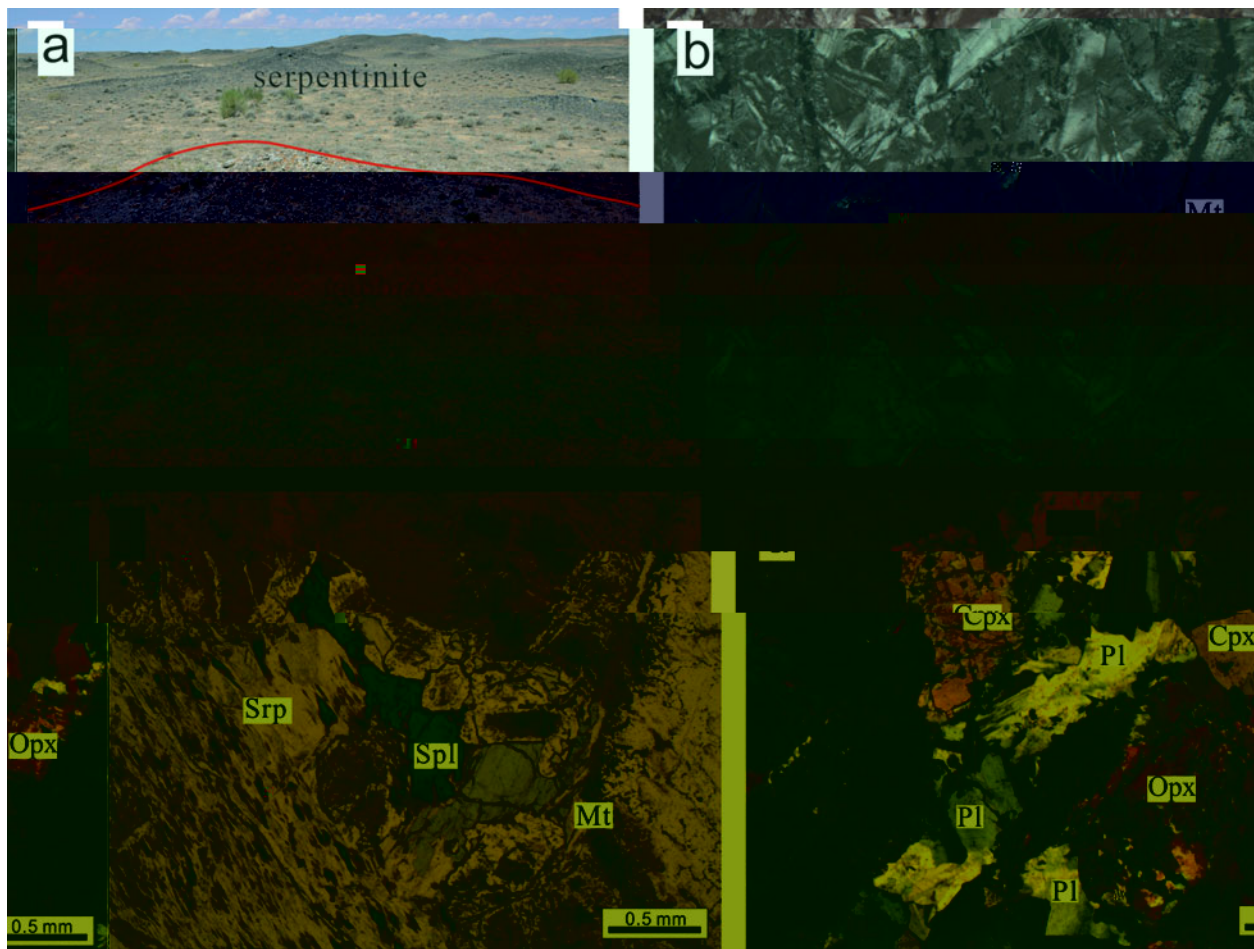


Figure 3. (a) Field view of serpentinite showing a fold (red line). (b) Photomicrograph of a rock with mineral grains labeled Opx, Pl, and Cpx. (c) Photomicrograph of a rock with mineral grains labeled Srp, Spl, Mt, and Opx. Scale bars are 0.5 mm.

	2013	01-1	2013	01-3	2013	01-4	2013	01-5	2013	01-6	2013	01-	2013	01-	2013	01. 1	2013	01. 2	2013	01. 4
<i>Major elements (%)</i>																				
SiO ₂	3.0	4.20	3.41	3.62	3.22	3.2	3.05	4.22	46.4	51.2										
TiO ₂	0.05	0.20	0.05	0.05	0.04	0.05	0.04	0.14	0.12	0.2										
Al ₂ O ₃	0.61	1.6	1.04	0.6	0.0	0.4	0.0	1.2	1.64	1.33										
Fe ₂ O ₃	.44	4.6	.	.36	.5	.16	.4	3.6	3.24	3.										
MnO	0.0	0.10	0.11	0.11	0.11	0.0	0.11	0.0	0.0	0.0										
MgO	3.21	24.5	3.2	3.	3.0	3.31	3.44	10.04	.03	5.										
20141.306 .201 () 1() 4 5(02 (30. (4 .20)-. (6-.501-)-60203(0. 0)-5)-60202.11)-602 .																				

Element

Element	2013 01-1	2013 01-3	2013 01-4	2013 01-5	2013 01-6	2013 01-	2013 01-1	2013 01-2	2013 01-4
	0.005	0.064	0.00	0.005	0.00	0.003	0.003	0.051	0.222
	0.021	0.34	0.044	0.042	0.0 2	0.031	0.033	0.310	1.450
	0.004	0.04	0.00	0.00	0.011	0.005	0.005	0.04	0.21
	0.011	0.232	0.036	0.044	0.012	0.034	0.00	0.123	0. 3
	0.0 0	0.036	0.03	0.03	0.06	0.026	0.025	0.046	0.06
	0.26	1. 10	6.600	1. 0	0. 3	0.233	1.150	1.5 0	0.1 5
	0.406	0.0 2	0.12	0.112	0.0	0.1	0.054	0.16	0.6 5
	0.046	0.034	0.014	0.02	0.050	0.030	0.010	0.050	0.130
	0.1 1	0.144	0.203	0.364	0.042	0.0 4	0.0	0.066	0.0 3

Element	2013 01. 5	2013 01. 6	2013 01. (1)	2013 01. (1)	2013 01. (1)	2013 03. 2 (1)	2013 03. 3 (1)	2013 03. 4 (1)	2013 03. 5 (1)	2013 01. 3 (2)
	4. 1	45.	4. 1	53.1	51. 1	50.40	50.54	50.52	51.22	52.3
	0.34	0.15	1.40	1.24	1.31	1. 0	1.63	1.31	1.1	0.33
	1. 1	1. 5	16.5	16.1	15. 3	15. 0	16. 6	15.55	15.4	1. 61
	4.52	3.34	. 11	. 11	. 43	. 0	. 50	. 42	. 2	3.44
	0.0	0.0	0.11	0.10	0.11	0.13	0.11	0.14	0.12	0.0
	6. 1	. 42	4. 0	4.2	4.41	5. 1	3.2	6.06	. 14	4. 1
	11.03	12.61	6.22	5. 5	6.3	6. 5	4.52	. 4	. 26	. 0
	4. 6	. 3	. 2	. 3	. 00	4.52	. 31	4. 0	4.0	. 11
	0.13	0.11	0.3	0.31	0.42	2.04	0.33	1.2	2.03	0.1
	0.04	0.02	0.62	0.62	0.65	0. 4	0.6	0.4	0.44	0.04
	3. 2	3.26	4.24	2.54	2. 3	2.2	5.14	2.65	1. 3	2. 1
	1. 5	1. 2	1. 6	1. 0	1. 4	1. 40	1. 1	1. 6	1. 6	1. 1
	4. 1	. 4	. 11	. 0	. 42	6.56	. 64	6.0	6.11	. 2
#	5	1	55	54	54	56	41	56	64	4

Element	2013 01. 5	2013 01. 6	2013 01. (1)	2013 01. (1)	2013 01. (1)	2013 03. 2 (1)	2013 03. 3 (1)	2013 03. 4 (1)	2013 03. 5 (1)	2013 01. 3 (2)
	0.0	4. 5	1.16	1.12	1.4	1.0	40.4	5.2	6. 2	5. 1
	0.22	0.135	1.2 4	1.6 3	1.316	1. 53	1.034	1.100	0.5 5	0.62
	25.0	23.	1. 6	1. 5	1. 5	. 5	1. 2	25.2	1. 1	1. 0
	11	3.	1. 6	166	1. 2	22	22	254	1	5.
	34.	163	60.5	62.6	64.1	116	1. 1	. 0	203	23.
	24.2	21.6	26.	23.6	24.6	2. 1	2. 5	2. 0	2. 0	16.4
	4.	1. 5	63.6	50.	51.4	6.	2. 1	5. 3	132	1.1

Table 1. ...

Sample No.	2013 01. 5	2013 01. 6	2013 01. 7	2013 01. 8	2013 01. 9	2013 03. 2	2013 03. 3	2013 03. 4	2013 03. 5	2013 01. 3
Age (Ma)	3.1	1.20	3.60	46.0	4.30	23.40	43.00	25.20	32.0	6.56

Element

Element	2013 (2)	01. 11 (2)	2013 (2)	02. 1 (2)	2013 (2)	02. 2 (2)	2013 (1)	03. 1 (1)	2013 (1)	03. 6 (1)	2013 (2)	01. 10 (2)	04 06 (1)	04 24 (1)	04 2 (1)	03 1 (1)
<i>Trace elements (ppm)</i>																
	1.4	36.	42.4	26.0	26.0	32.4	1.	/	/	/	/	/	/	/	/	/
	0.3 5	0.153	0.35	1.1	0.4	0.46	1.1	/	/	/	/	/	/	/	/	/
	32.5	33.2	34.5	25.1	26.3	32.1	13.4	20.5	1.	20.3						
	1.4	203	21	33	341	1.5	144	1.4	214	265						
	56.5	44.2	4.	1.	22.2	53.	15	162	214	265						
	34.	3.5	3.3	23.1	24.	33.	20.6	30.	2.	20.2						
	66.4	4.6	6.4	25.4	2.1	66.6	.1	114	5.5	.02						
	6.4	236.4	256.	205.4	20.	114.20	/	/	/	/						
	4.0	44.1	4.0	4.	103	44.1	/	/	/	/						
	12.0	11.1	11.2	14.	13.6	12.0	/	/	/	/						
	0.5	1.420	1.0 0	3.130	3.2 0	0.5 3	4.	1.1	22.0	1.2						
	.1	1.50	.5	2.0	24.	6.6	.1	31	111	.6						
	13.0	13.0	13.2	21.1	22.	12.5	13.2	13.2	14.	20.1						
	54.	42.3	41.5	144	154	52.	243	133	164	151						
	1.2	0.4	0.55	11.315	11.5	1.25	20.2	12.	21.	12.2						
	0.025	0.030	0.02	0.051	0.052	0.02	/	/	/	/						
	0.3 1	0.2 6	0.32	1.560	1.450	0.360	/	/	/	/						
	0.2	1.20	1.030	0.365	0.406	0.336	/	/	/	/						
	11	3.2	346	25	50	4.3	/	/	/	/						
	10.0	.40	.610	26.40	26.0	10.50	30.6	32.2	40.1	26.4						
	23.00	1.0	1.40	51.50	54.0	22.30	5.	62.	2.3	52.5						
	2.0	2.520	2.510	5.50	6.1 0	2.6 0	6.	.4	10.5	6.4						
	11.0	11.0	11.60	22.30	24.30	11.60	2.5	31.2	43.1	24.4						
	2.540	2.00	2.6 0	4.4 0	4.00	2.3 0	4.5	5.2	6.	4.5						
	0.6	0.1	0.0	1.163	1.25	0.3	1.45	1.5	2.0	1.03						
	2.4 0	2.13	2.54	4.14	4.46	2.522	3.56	4.01	5.35	4.23						
	0.3 6	0.3	0.3	0.612	0.660	0.3 4	0.4	0.54	0.64	0.63						
%	2.1 0	2.150	2.220	3.420	3.6 0	2.130	2.5	2.	3.24	3.5						
	0.46	0.446	0.444	0.2	0.5	0.46	0.4	0.52	0.5	0.						
	1.350	1.230	1.240	2.120	2.2 0	1.310	1.32	1.3	1.45	2.25						
	0.1 0	0.16	0.1 5	0.304	0.32	0.1 4	0.1	0.2	0.2	0.34						
	1.210	1.050	1.120	1.60	2.110	1.210	1.25	1.23	1.24	2.13						
	0.1 4	0.164	0.165	0.2 1	0.323	0.1 3	0.20	0.1	0.1	0.34						
	1.3 0	0.41	1.040	3.2 0	3.510	1.460	5.3	3.2	4.16	3.2						
	0.0 4	0.062	0.051	0.5	0.644	0.0	1.35	0.6	1.16	0.6						
	0.151	2.0	1.50	2.5	1.	0.33	/	/	/	/						
	0.3 4	0.206	0.200	45.20	35.10	0.41	.13	.0	4.1	21.06						
	1.0	0.61	0.1	.60	.2 0	1.0	4.50	2.63	3.20	.41						
	0.500	0.304	0.302	2.30	3.4 0	0.501	1.	0.6	1.46	2.5						

Element / ... et al. (200 a).

Table 2. U-Pb zircon ages and ϵ_{Pb} values of the Zhaheba ophiolite.

Year	Sample	Grains	ϵ_{Pb}	$^{206}\text{Pb}/^{238}\text{U}$	$^{207}\text{Pb}/^{235}\text{U}$	$^{206}\text{Pb}/^{238}\text{U}$	$^{207}\text{Pb}/^{235}\text{U}$	$^{206}\text{Pb}/^{238}\text{U}$	$^{207}\text{Pb}/^{235}\text{U}$	^{14}C	^{143}C	$^{143}\text{C}/^{144}\text{C}$	ϵ_{Pb}
2013	01.3	2	0.36	3.2	0.002	0.04030(2)	0.04015	2.4	10.	0.134	0.5123	(40)	0.51244
2013	01.10	2	0.5	6.6	0.0024	0.045(23)	0.0445	2.3	11.6	0.1235	0.5120	(43)	0.51246
2013	03.1	1	3.13	2.0	0.0335	0.06324(20)	0.06133	4.4	22.3	0.121	0.512533(4)	(51)	0.512214
2013	03.2	1	2.	1320	0.0063	0.042(20)	0.04255	4.5	2.6	0.1046	0.5121	(30)	0.512445
2013	03.3	1	0.06	516	0.0452	0.0536(43)	0.05111	5.	36.	0.0	0.5120	(30)	0.512450
2013	03.4	1	0.65	140	0.01	0.0422(51)	0.04120	4.55	24.5	0.1123	0.51203(53)	(51)	0.51250

$\epsilon_{\text{Pb}}(t) = 10000 \left(\frac{^{143}\text{C}/^{144}\text{C}}{^{143}\text{C}/^{144}\text{C}}(t) - 1 \right)$ $\epsilon_{\text{Pb}}(t) = \left(\frac{^{206}\text{Pb}/^{238}\text{U}}{^{206}\text{Pb}/^{238}\text{U}}(t) - 1 \right) \times 10^4$

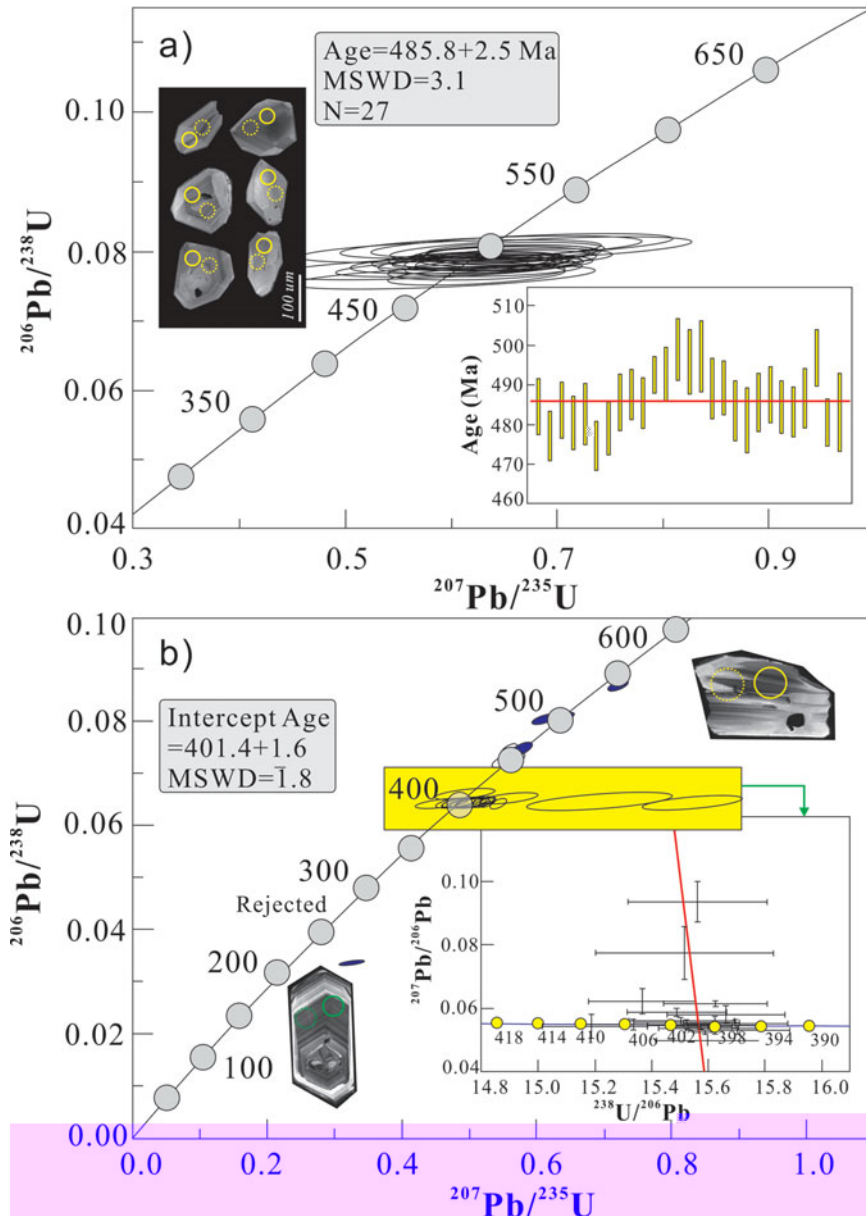


Figure 4. U-Pb zircon age spectra of the Zhaheba ophiolite. (a) Age spectrum of sample 01.3, showing a linear array of data points with an age of 485.8 ± 2.5 Ma, MSWD=3.1, N=27. (b) Age spectrum of sample 01.10, showing a linear array of data points with an intercept age of 401.4 ± 1.6 Ma, MSWD=1.8.

($n = 2$, $\sigma = 3.1$). The age spectrum of sample 01.10 shows a linear array of data points with an intercept age of 401.4 ± 1.6 Ma, MSWD=1.8. The age spectrum of sample 03.1 shows a linear array of data points with an age of 632.4 ± 2.0 Ma, MSWD=20. The age spectrum of sample 03.2 shows a linear array of data points with an age of 42.0 ± 0.0063 Ma, MSWD=20. The age spectrum of sample 03.3 shows a linear array of data points with an age of 53.6 ± 0.05111 Ma, MSWD=43. The age spectrum of sample 03.4 shows a linear array of data points with an age of 42.2 ± 0.04120 Ma, MSWD=51.

...%, ... (2, ... 4).
 ... 1e. ... 1 ... 2
 ... 450. ...
 500. ...
 21 ... 1 ...
 206 23 ...
 401 ± 2 ... $= 3.3$...
 206 23 ... 20 235 ...
 401.4 ± 1.6 ... $= 1.$...
 ... 4), ... 206
 23 ...
 ... 1.3).

4.b. M a c

4.b.1. Spinel composition

...% ... 1e ...
 (... 3). ... 100 - 300 μ ...
 ...% ... 11e ...% ...
 4 ... 1 // ... / e)
 ... 1e ... 2 3, e ... 2 3 ...
 ...% ... 1e ...% 1e
 ... 1e ... (100 / (+))
 ... 44 60 ... (100 / (+ e))
 ... 25 61. ... 1 ...
 ... / e ... /
 1 - ... et al. 2010). ...
 ... () ... 1 ...
 ... 1 ...
 ... et al. 2013).

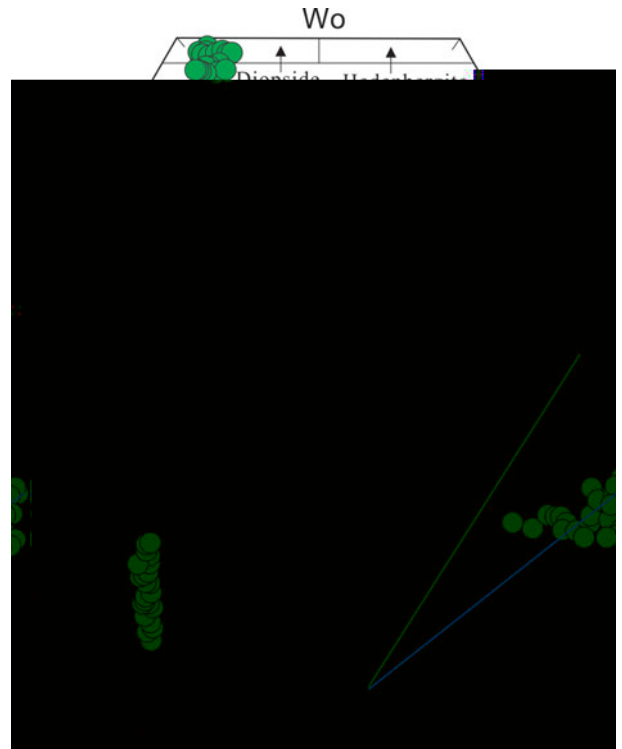
4.b.2. Pyroxene compositions

... 1% ... e ...
 ... e ... 1 ... = 4 6). ...
 ... 1% ... % ...
 ... (e ... 0.5%) ... 1 -
 ... 1e (... 11e-
 ... 5 ... 1 // ...
 ... / e). ... 1% ...
 ... 1 ...
 41 4 ... 46 55 ... 1
 (... 5). ...
 ... e ... e ...
 ... 2 3, ... 2 ... 2 ...
 (... 5, e).

4.c. W - c a c

4.c.1. Serpentinites and cumulates

...e ... e ...% ... ()
 (> 12%, ... e ... e ...
 ...) ... 2 (e ... 40%), ... 2 3 (... %
 ... 1.0%), ... 2 (0.03 0.06%), ... 2 (0.04
 0. 2%) ... 2 (0.04 0.05%). ... e 2 3 ...



...e 5. (... e) () ...
 ... 1 ... 1% ...
 ... 1 ... 2 (%) ... 2 3 (%) ... (e)
 (1e ... e ... e ... 1e ... %) ... 2 (%)
 ... 1% ... e ... 1 ...

e ... 1 (e 1) ...
 ... e ... e ... e ...
 ... e ... e ... (.6).
 ...% ... (3 103 11) ...
 ... (5 11) (e 1). ... (> 12%)
 ... 2 , 2 ... e ...
 ...% ... e ... e ...
 ... e ... e ... (,) ...
 ... 1 ... () (e. ,
 ...) ... e , ... e ...
 ... , 2 3, e 2 3 ... 2, e
 ... e ... % ...
 ... e ... e ... le -
 ... e ... e ...
 ... () ... - e - e ...
 ...) ... (e 1). ... e% ...
 ... - 1e ... e ... 1e
 (...), ... e ...
 1 ... 1e (... 2014 ... e
 ... e 1 ... e ... & e
 ... , 1 ...).

... e ... e ... 2 ...
 45. % 51.2 %, ... 1% ...
 e 2 3 (3.24 4.6 %), ... 2 3 (1.3 1.6%, e ...
 ... 1e 2013 01-3), ... (.54 15.42%), ... 2
 (0.12 0.34%), ... 2 (2.1 3 %, e ... 1e
 2013 01-3) ... 2 (0.11 0.46%) ... e % -
 ... / e , ... e ... (e 1).

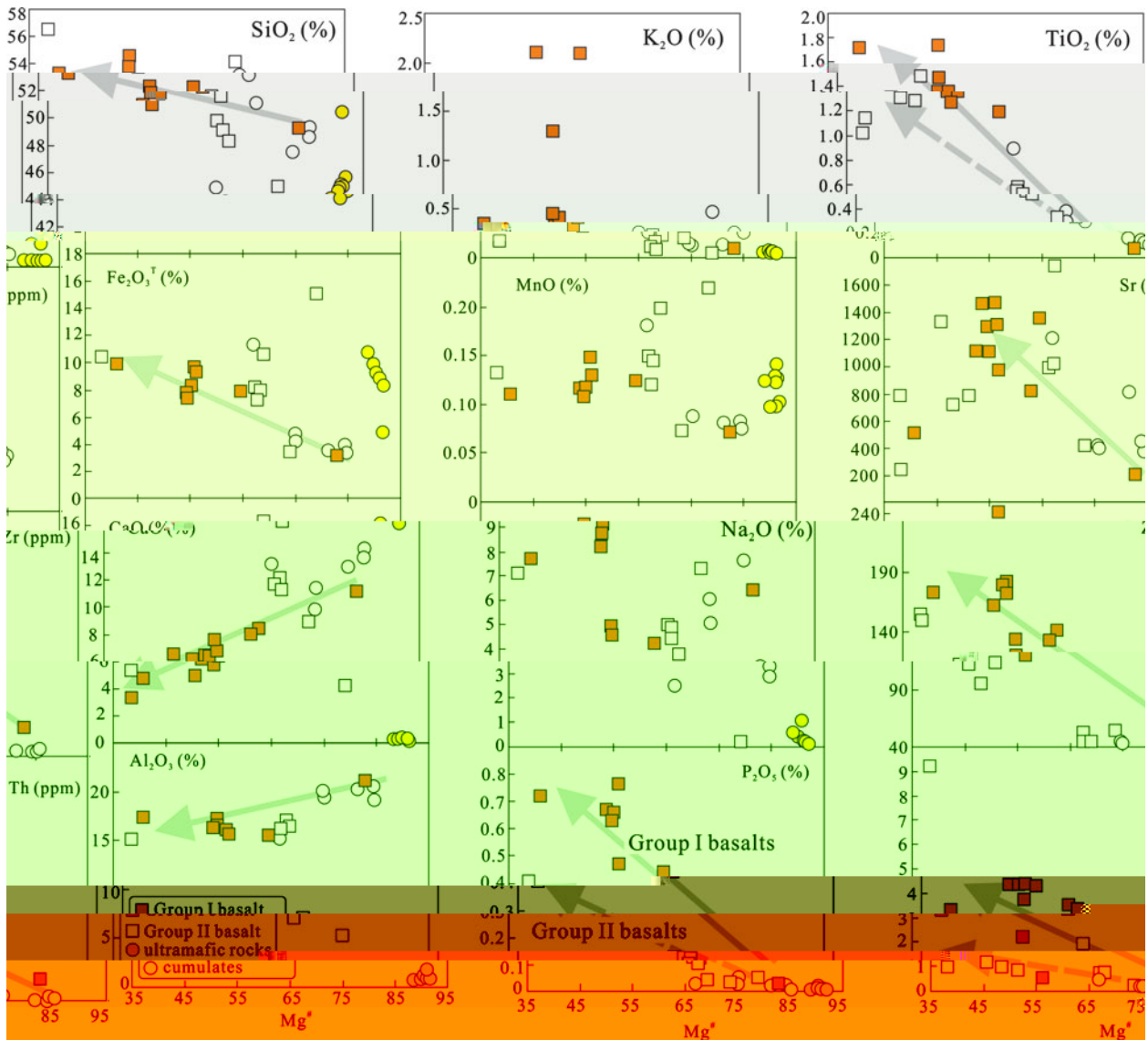


Figure 6. (a) (b) (c) (d) (e) (f) (g) (h) (i) (j) (k) (l) (m) (n) (o) (p) (q) (r) (s) (t) (u) (v) (w) (x) (y) (z) (aa) (ab) (ac) (ad) (ae) (af) (ag) (ah) (ai) (aj) (ak) (al) (am) (an) (ao) (ap) (aq) (ar) (as) (at) (au) (av) (aw) (ax) (ay) (az) (ba) (bb) (bc) (bd) (be) (bf) (bg) (bh) (bi) (bj) (bk) (bl) (bm) (bn) (bo) (bp) (bq) (br) (bs) (bt) (bu) (bv) (bw) (bx) (by) (bz) (ca) (cb) (cc) (cd) (ce) (cf) (cg) (ch) (ci) (cj) (ck) (cl) (cm) (cn) (co) (cp) (cq) (cr) (cs) (ct) (cu) (cv) (cw) (cx) (cy) (cz) (da) (db) (dc) (dd) (de) (df) (dg) (dh) (di) (dj) (dk) (dl) (dm) (dn) (do) (dp) (dq) (dr) (ds) (dt) (du) (dv) (dw) (dx) (dy) (dz) (ea) (eb) (ec) (ed) (ee) (ef) (eg) (eh) (ei) (ej) (ek) (el) (em) (en) (eo) (ep) (eq) (er) (es) (et) (eu) (ev) (ew) (ex) (ey) (ez) (fa) (fb) (fc) (fd) (fe) (ff) (fg) (fh) (fi) (fj) (fk) (fl) (fm) (fn) (fo) (fp) (fq) (fr) (fs) (ft) (fu) (fv) (fw) (fx) (fy) (fz) (ga) (gb) (gc) (gd) (ge) (gf) (gg) (gh) (gi) (gj) (gk) (gl) (gm) (gn) (go) (gp) (gq) (gr) (gs) (gt) (gu) (gv) (gw) (gx) (gy) (gz) (ha) (hb) (hc) (hd) (he) (hf) (hg) (hh) (hi) (hj) (hk) (hl) (hm) (hn) (ho) (hp) (hq) (hr) (hs) (ht) (hu) (hv) (hw) (hx) (hy) (hz) (ia) (ib) (ic) (id) (ie) (if) (ig) (ih) (ii) (ij) (ik) (il) (im) (in) (io) (ip) (iq) (ir) (is) (it) (iu) (iv) (iw) (ix) (iy) (iz) (ja) (jb) (jc) (jd) (je) (jf) (jg) (jh) (ji) (jj) (jk) (jl) (jm) (jn) (jo) (jp) (jq) (jr) (js) (jt) (ju) (jv) (jw) (jx) (jy) (jz) (ka) (kb) (kc) (kd) (ke) (kf) (kg) (kh) (ki) (kj) (kk) (kl) (km) (kn) (ko) (kp) (kq) (kr) (ks) (kt) (ku) (kv) (kw) (kx) (ky) (kz) (la) (lb) (lc) (ld) (le) (lf) (lg) (lh) (li) (lj) (lk) (ll) (lm) (ln) (lo) (lp) (lq) (lr) (ls) (lt) (lu) (lv) (lw) (lx) (ly) (lz) (ma) (mb) (mc) (md) (me) (mf) (mg) (mh) (mi) (mj) (mk) (ml) (mm) (mn) (mo) (mp) (mq) (mr) (ms) (mt) (mu) (mv) (mw) (mx) (my) (mz) (na) (nb) (nc) (nd) (ne) (nf) (ng) (nh) (ni) (nj) (nk) (nl) (nm) (nn) (no) (np) (nq) (nr) (ns) (nt) (nu) (nv) (nw) (nx) (ny) (nz) (oa) (ob) (oc) (od) (oe) (of) (og) (oh) (oi) (oj) (ok) (ol) (om) (on) (oo) (op) (oq) (or) (os) (ot) (ou) (ov) (ow) (ox) (oy) (oz) (pa) (pb) (pc) (pd) (pe) (pf) (pg) (ph) (pi) (pj) (pk) (pl) (pm) (pn) (po) (pp) (pq) (pr) (ps) (pt) (pu) (pv) (pw) (px) (py) (pz) (qa) (qb) (qc) (qd) (qe) (qf) (qg) (qh) (qi) (qj) (qk) (ql) (qm) (qn) (qo) (qp) (qq) (qr) (qs) (qt) (qu) (qv) (qw) (qx) (qy) (qz) (ra) (rb) (rc) (rd) (re) (rf) (rg) (rh) (ri) (rj) (rk) (rl) (rm) (rn) (ro) (rp) (rq) (rr) (rs) (rt) (ru) (rv) (rw) (rx) (ry) (rz) (sa) (sb) (sc) (sd) (se) (sf) (sg) (sh) (si) (sj) (sk) (sl) (sm) (sn) (so) (sp) (sq) (sr) (ss) (st) (su) (sv) (sw) (sx) (sy) (sz) (ta) (tb) (tc) (td) (te) (tf) (tg) (th) (ti) (tj) (tk) (tl) (tm) (tn) (to) (tp) (tq) (tr) (ts) (tt) (tu) (tv) (tw) (tx) (ty) (tz) (ua) (ub) (uc) (ud) (ue) (uf) (ug) (uh) (ui) (uj) (uk) (ul) (um) (un) (uo) (up) (uq) (ur) (us) (ut) (uu) (uv) (uw) (ux) (uy) (uz) (va) (vb) (vc) (vd) (ve) (vf) (vg) (vh) (vi) (vj) (vk) (vl) (vm) (vn) (vo) (vp) (vq) (vr) (vs) (vt) (vu) (vv) (vw) (vx) (vy) (vz) (wa) (wb) (wc) (wd) (we) (wf) (wg) (wh) (wi) (wj) (wk) (wl) (wm) (wn) (wo) (wp) (wq) (wr) (ws) (wt) (wu) (wv) (ww) (wx) (wy) (wz) (xa) (xb) (xc) (xd) (xe) (xf) (xg) (xh) (xi) (xj) (xk) (xl) (xm) (xn) (xo) (xp) (xq) (xr) (xs) (xt) (xu) (xv) (xw) (xx) (xy) (xz) (ya) (yb) (yc) (yd) (ye) (yf) (yg) (yh) (yi) (yj) (yk) (yl) (ym) (yn) (yo) (yp) (yq) (yr) (ys) (yt) (yu) (yv) (yw) (yx) (yy) (yz) (za) (zb) (zc) (zd) (ze) (zf) (zg) (zh) (zi) (zj) (zk) (zl) (zm) (zn) (zo) (zp) (zq) (zr) (zs) (zt) (zu) (zv) (zw) (zx) (zy) (zz)

... (6) ...
 ... 511 ... 4111 ...
 ...
 ... ((/) = 1.3 2.)
 ... (/ , = 1.1 2.2).
 ... 2013 01-3 ...
 ... % ...
 ...
 ...
 ...
 ...
 ...
 ... (/ = 0.2 0.4)
 ...

4.c.2. Basalts

... 43.15% ... 5.65% (% e ... 52%,

... (e1). ... % ...
 ...
 ... / ... / 2 ...
 ... 11 (1) ... 12 (2).
 ... 2 ... 1e, ... 1e ...
 ... % ...
 ... (...) ...
 ... 2, e2 3, 2 5, ...
 ... 2 3 ...
 ... 1 ... 2 ...
 ... 2 5, ...
 ... (...) ...

... (6).
 ... 1 ... % ...
 ... 124 11 ... 205 11 ... e e 2 ...
 ... 50 11 ... 60 11 ... 1 ...
 ... (/) ... e e 10 ...
 ... 30 (% ... e 20) ...

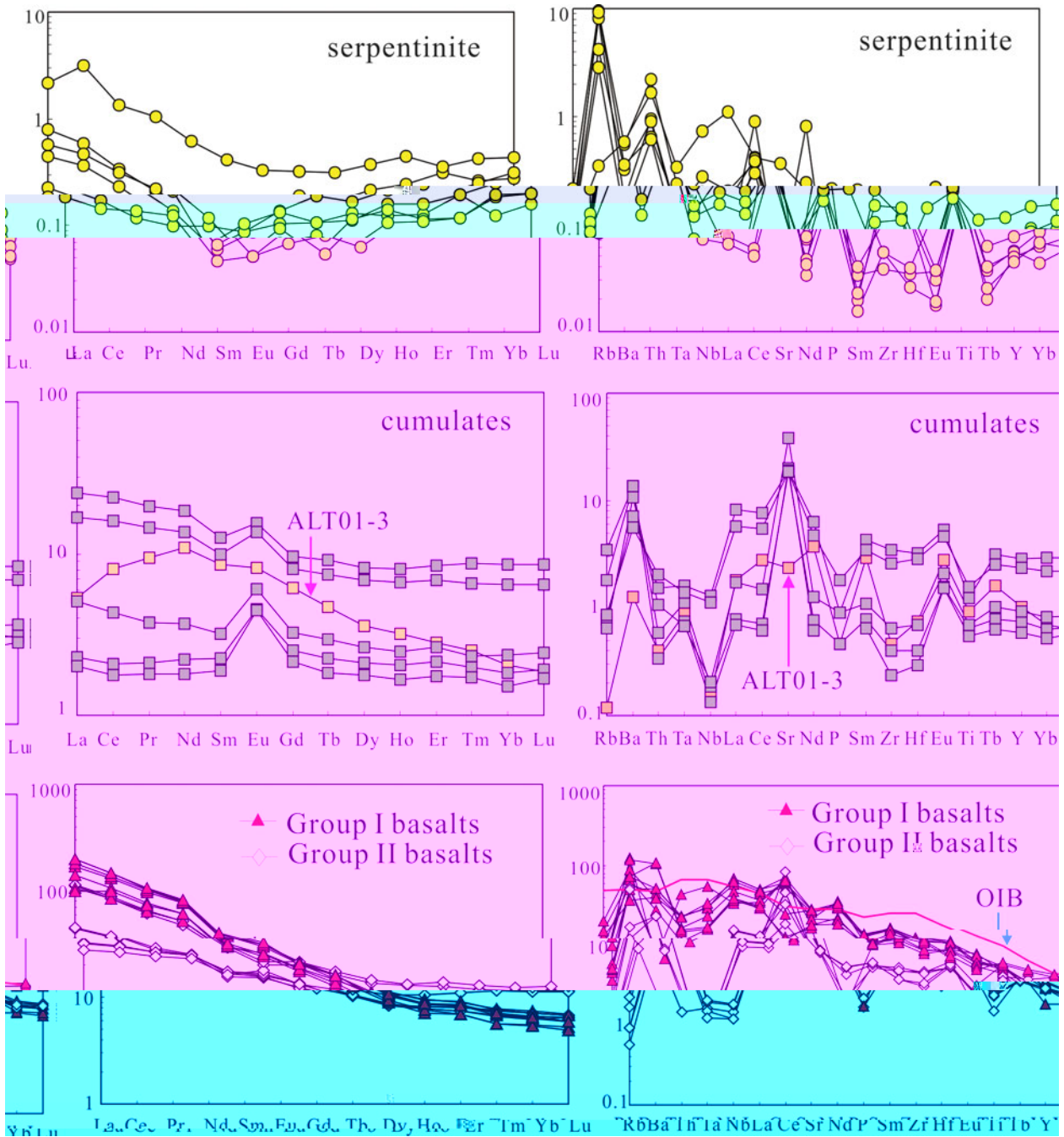


Fig. 1. REE and trace element patterns for serpentinite, cumulates and basalts. The top row shows REE patterns for serpentinite, the middle row shows REE patterns for cumulates, and the bottom row shows REE patterns for Group I and Group II basalts. The OIB pattern is shown for comparison. The x-axis represents the REE elements (La, Ce, Pr, Nd, Sm, Eu, Gd, Tb, Dy, Ho, Er, Tm, Yb, Lu) and the y-axis represents the concentration in ppm on a log scale. The bottom right plot also includes trace elements Rb, Ba, Th, Ta, Nb, La, Ce, Sr, Nd, P, Sm, Zr, Hf, Eu, Ti, Tb, Y.

1. The REE patterns for serpentinite (Fig. 1) show a characteristic enrichment in light REE, with (La/Sm)_N = 0.0–1.14 (n = 2) and (Ce/Sm)_N = 0.4–1.4 (n = 4). The patterns for cumulates (Fig. 1) show a similar enrichment in light REE, with (La/Sm)_N = 1.02–1.21 (n = 1) and (Ce/Sm)_N = 0.44–0.8 (n = 1). The REE patterns for Group I basalts (Fig. 1) show a characteristic enrichment in light REE, with (La/Sm)_N = 0.0–1.14 (n = 1) and (Ce/Sm)_N = 0.4–1.4 (n = 1). The REE patterns for Group II basalts (Fig. 1) show a characteristic enrichment in light REE, with (La/Sm)_N = 0.0–1.14 (n = 1) and (Ce/Sm)_N = 0.4–1.4 (n = 1).

4. The REE patterns for Group I basalts (Fig. 1) show a characteristic enrichment in light REE, with (La/Sm)_N = 0.0–1.14 (n = 1) and (Ce/Sm)_N = 0.4–1.4 (n = 1). The REE patterns for Group II basalts (Fig. 1) show a characteristic enrichment in light REE, with (La/Sm)_N = 0.0–1.14 (n = 1) and (Ce/Sm)_N = 0.4–1.4 (n = 1). The OIB pattern (Fig. 1) shows a characteristic enrichment in light REE, with (La/Sm)_N = 0.0–1.14 (n = 1) and (Ce/Sm)_N = 0.4–1.4 (n = 1).

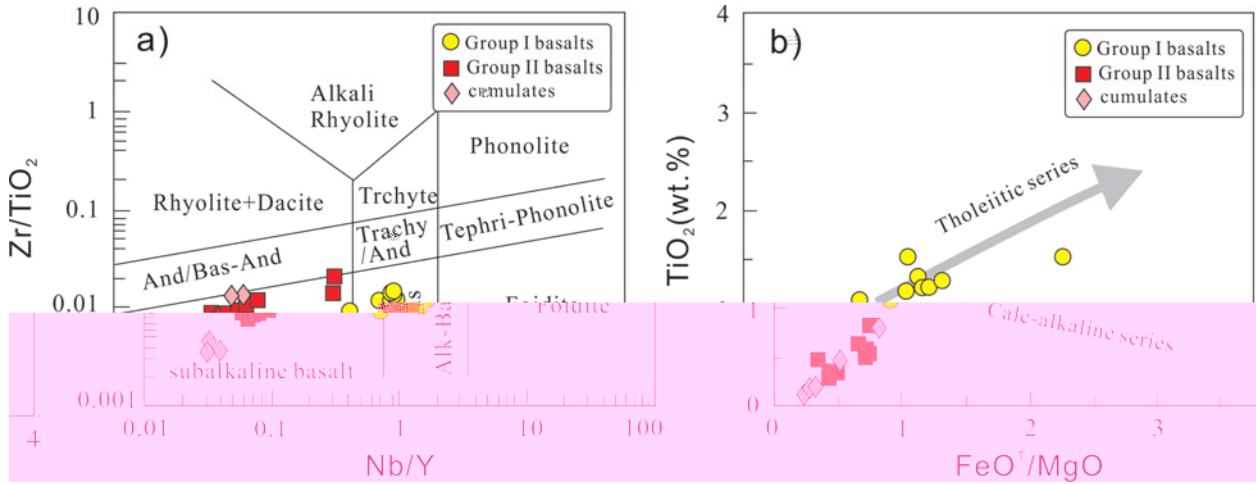


Fig. 1. Geochemical diagrams for Group I basalts (yellow circles), Group II basalts (red squares), and cumulates (red diamonds). (a) Zr/TiO₂ vs Nb/Y diagram showing various rock fields. (b) TiO₂ vs FeO^T/MgO diagram showing Tholeiitic and Calc-alkaline series. Shaded areas indicate subalkaline basalt and Alk-Bas fields.

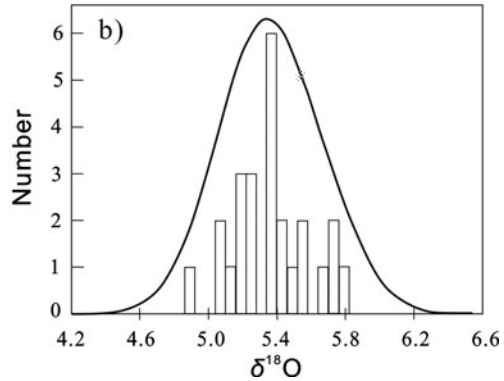
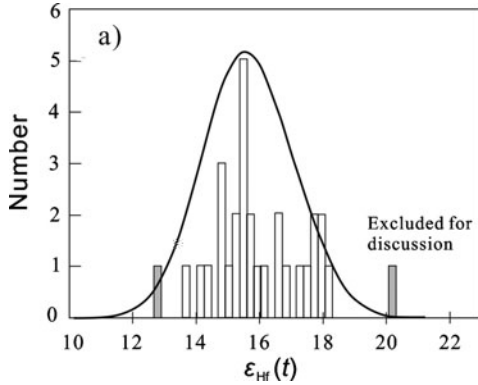


Fig. 2. Histograms of ε_{Hf}(t) (a) and δ¹⁸O (b) for Group I basalts. Normal distribution curves are overlaid on the histograms.

The ε_{Hf}(t) values for Group I basalts range from 13.2 to 20.1‰, with a mean of 15.1 ± 1.2‰ (n = 11). One sample (Zhaheba-4) with ε_{Hf}(t) = 20.1‰ is excluded for discussion. The δ¹⁸O values range from 4.9‰ to 5.8‰, with a mean of 5.3 ± 0.23‰ (n = 11).

5. Discussion
5.a. Textural and geochemical features of the Zhaheba ophiolite
 The Zhaheba ophiolite consists of a sequence of mafic rocks including gabbro, diorite, and basalt. The gabbro is characterized by a coarse-grained texture with large plagioclase crystals. The diorite has a fine-grained texture with plagioclase and quartz. The basalt shows a variety of textures, including aphyric, micritic, and porphyritic. The geochemical features of the basalts are discussed in detail in the text.

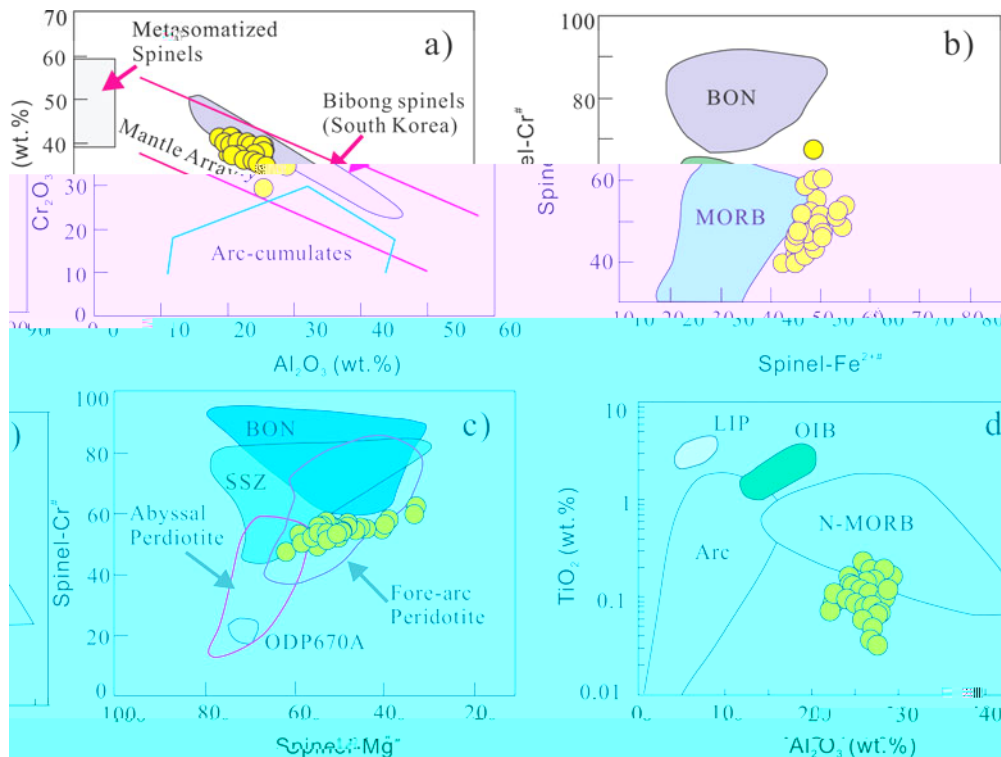


Fig. 10. (a) Cr_2O_3 vs Al_2O_3 (wt.%) diagram showing the composition of spinels from the Mantle Array (Mantle Array) and Bibong spinels (South Korea) (Bibong spinels (South Korea)). The field for Metasomatized Spinel is also shown. (b) $Spinel-Fe^{2+}$ vs $Spinel-Cr^{\#}$ diagram showing the composition of spinels from the Mantle Array (Mantle Array) and Bibong spinels (South Korea) (Bibong spinels (South Korea)). The fields for BON and MORB are also shown. (c) $Spinel-Cr^{\#}$ vs $Spinel-Mg^{\#}$ diagram showing the composition of spinels from the Mantle Array (Mantle Array) and Bibong spinels (South Korea) (Bibong spinels (South Korea)). The fields for BON, SSZ, Abyssal Peridotite, and Fore-arc Peridotite are also shown. (d) TiO_2 (wt.%) vs Al_2O_3 (wt.%) diagram showing the composition of spinels from the Mantle Array (Mantle Array) and Bibong spinels (South Korea) (Bibong spinels (South Korea)). The fields for LIP, OIB, N-MORB, and Arc are also shown.

Fig. 10. (a) Cr_2O_3 vs Al_2O_3 (wt.%) diagram showing the composition of spinels from the Mantle Array (Mantle Array) and Bibong spinels (South Korea) (Bibong spinels (South Korea)). The field for Metasomatized Spinel is also shown. (b) $Spinel-Fe^{2+}$ vs $Spinel-Cr^{\#}$ diagram showing the composition of spinels from the Mantle Array (Mantle Array) and Bibong spinels (South Korea) (Bibong spinels (South Korea)). The fields for BON and MORB are also shown. (c) $Spinel-Cr^{\#}$ vs $Spinel-Mg^{\#}$ diagram showing the composition of spinels from the Mantle Array (Mantle Array) and Bibong spinels (South Korea) (Bibong spinels (South Korea)). The fields for BON, SSZ, Abyssal Peridotite, and Fore-arc Peridotite are also shown. (d) TiO_2 (wt.%) vs Al_2O_3 (wt.%) diagram showing the composition of spinels from the Mantle Array (Mantle Array) and Bibong spinels (South Korea) (Bibong spinels (South Korea)). The fields for LIP, OIB, N-MORB, and Arc are also shown.

5.b. O

Fig. 10. (a) Cr_2O_3 vs Al_2O_3 (wt.%) diagram showing the composition of spinels from the Mantle Array (Mantle Array) and Bibong spinels (South Korea) (Bibong spinels (South Korea)). The field for Metasomatized Spinel is also shown. (b) $Spinel-Fe^{2+}$ vs $Spinel-Cr^{\#}$ diagram showing the composition of spinels from the Mantle Array (Mantle Array) and Bibong spinels (South Korea) (Bibong spinels (South Korea)). The fields for BON and MORB are also shown. (c) $Spinel-Cr^{\#}$ vs $Spinel-Mg^{\#}$ diagram showing the composition of spinels from the Mantle Array (Mantle Array) and Bibong spinels (South Korea) (Bibong spinels (South Korea)). The fields for BON, SSZ, Abyssal Peridotite, and Fore-arc Peridotite are also shown. (d) TiO_2 (wt.%) vs Al_2O_3 (wt.%) diagram showing the composition of spinels from the Mantle Array (Mantle Array) and Bibong spinels (South Korea) (Bibong spinels (South Korea)). The fields for LIP, OIB, N-MORB, and Arc are also shown.

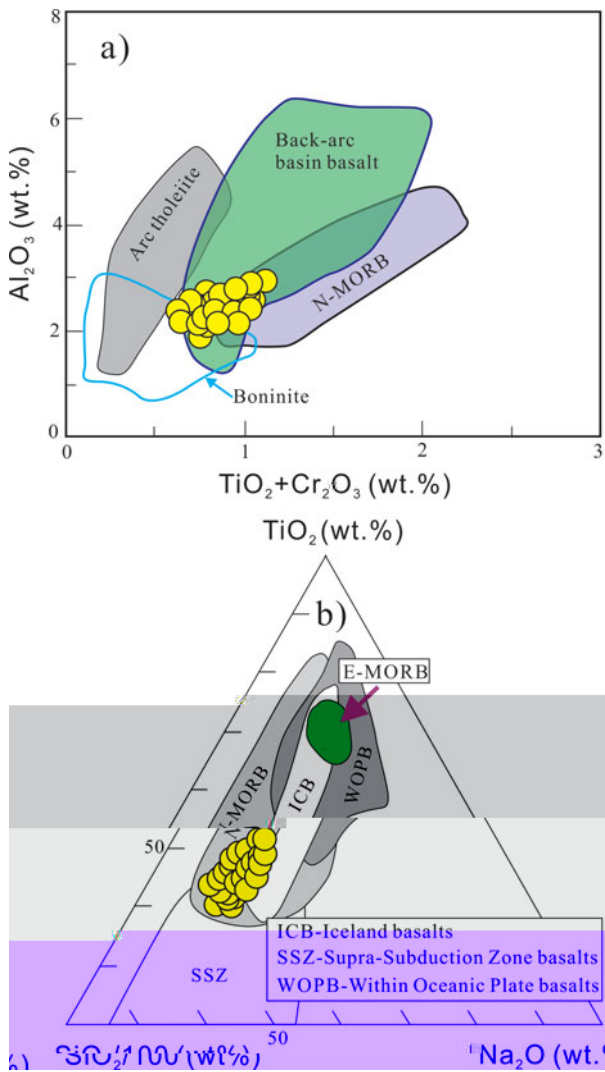


Fig. 11. (a) Al_2O_3 vs $TiO_2 + Cr_2O_3$ and TiO_2 diagram. (b) TiO_2 vs Na_2O vs CaO diagram. The fields are after [11].

The Zhaheba ophiolite is characterized by high Al_2O_3 content (2.5-3.5 wt.%) and low $TiO_2 + Cr_2O_3$ content (0.8-1.2 wt.%) (Fig. 11a). This composition is consistent with an arc tholeiite or back-arc basin basalt. The ternary diagram (Fig. 11b) shows that the Zhaheba ophiolite falls within the N-MORB field, indicating a mid-ocean ridge basalt origin. The presence of ICB (Icelandic basalts) and SSZ (Supra-Subduction Zone) basalts in the diagram suggests a tectonic setting related to subduction.

The geochemical characteristics of the Zhaheba ophiolite are consistent with a mid-ocean ridge basalt (MORB) origin. The high Al_2O_3 content and low $TiO_2 + Cr_2O_3$ content are typical of arc tholeiites and back-arc basin basalts. The ternary diagram (Fig. 11b) shows that the Zhaheba ophiolite falls within the N-MORB field, indicating a mid-ocean ridge basalt origin. The presence of ICB (Icelandic basalts) and SSZ (Supra-Subduction Zone) basalts in the diagram suggests a tectonic setting related to subduction.

5.c. P D a b a

The Zhaheba ophiolite is characterized by high Al_2O_3 content (2.5-3.5 wt.%) and low $TiO_2 + Cr_2O_3$ content (0.8-1.2 wt.%) (Fig. 11a). This composition is consistent with an arc tholeiite or back-arc basin basalt. The ternary diagram (Fig. 11b) shows that the Zhaheba ophiolite falls within the N-MORB field, indicating a mid-ocean ridge basalt origin. The presence of ICB (Icelandic basalts) and SSZ (Supra-Subduction Zone) basalts in the diagram suggests a tectonic setting related to subduction.

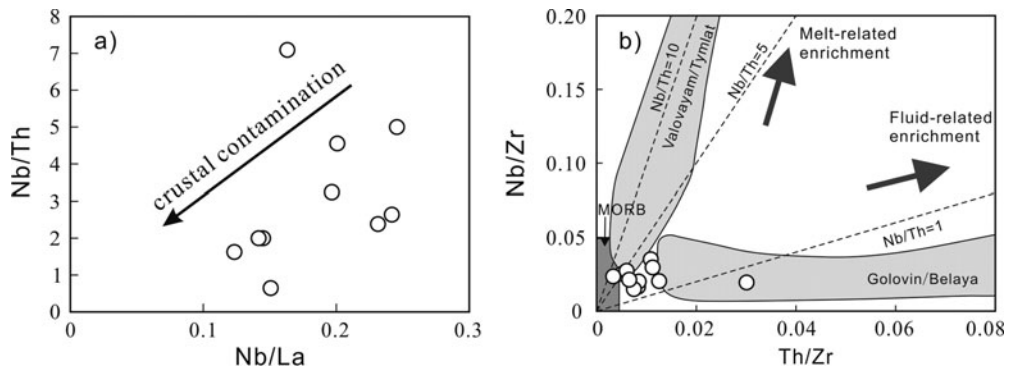


Fig. 12. (a) Nb/Th vs Nb/La (cf. Fig. 11b) showing the trend of crustal contamination. (b) Nb/Zr vs Th/Zr (cf. Fig. 11c) showing the trend of melt- and fluid-related enrichment.

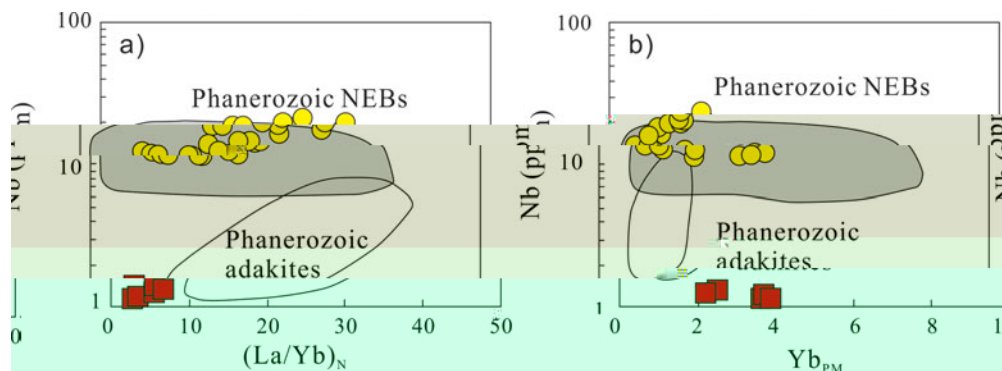


Fig. 13. (a) ϵ_{Nb} vs $(\text{La}/\text{Yb})_{\text{N}}$ (cf. Fig. 11b) showing the trend of crustal contamination. (b) ϵ_{Nb} vs Yb_{PM} (cf. Fig. 11c) showing the trend of melt- and fluid-related enrichment.

Figure 14. (a) ϵ_{Nb} vs $(\text{La}/\text{Yb})_{\text{N}}$ (cf. Fig. 11b) showing the trend of crustal contamination. (b) ϵ_{Nb} vs Yb_{PM} (cf. Fig. 11c) showing the trend of melt- and fluid-related enrichment. The fields for Phanerozoic NEBs and adakites are shown. The data points are represented by yellow circles and red squares. The y-axis is ϵ_{Nb} (‰) on a log scale from 1 to 100. The x-axis is $(\text{La}/\text{Yb})_{\text{N}}$ from 0 to 50. The y-axis is Yb_{PM} from 0 to 10. The x-axis is Yb_{PM} from 0 to 10. The fields for Phanerozoic NEBs and adakites are shown.

(Figure 14). The data points are represented by yellow circles and red squares. The y-axis is ϵ_{Nb} (‰) on a log scale from 1 to 100. The x-axis is $(\text{La}/\text{Yb})_{\text{N}}$ from 0 to 50. The y-axis is Yb_{PM} from 0 to 10. The x-axis is Yb_{PM} from 0 to 10. The fields for Phanerozoic NEBs and adakites are shown.

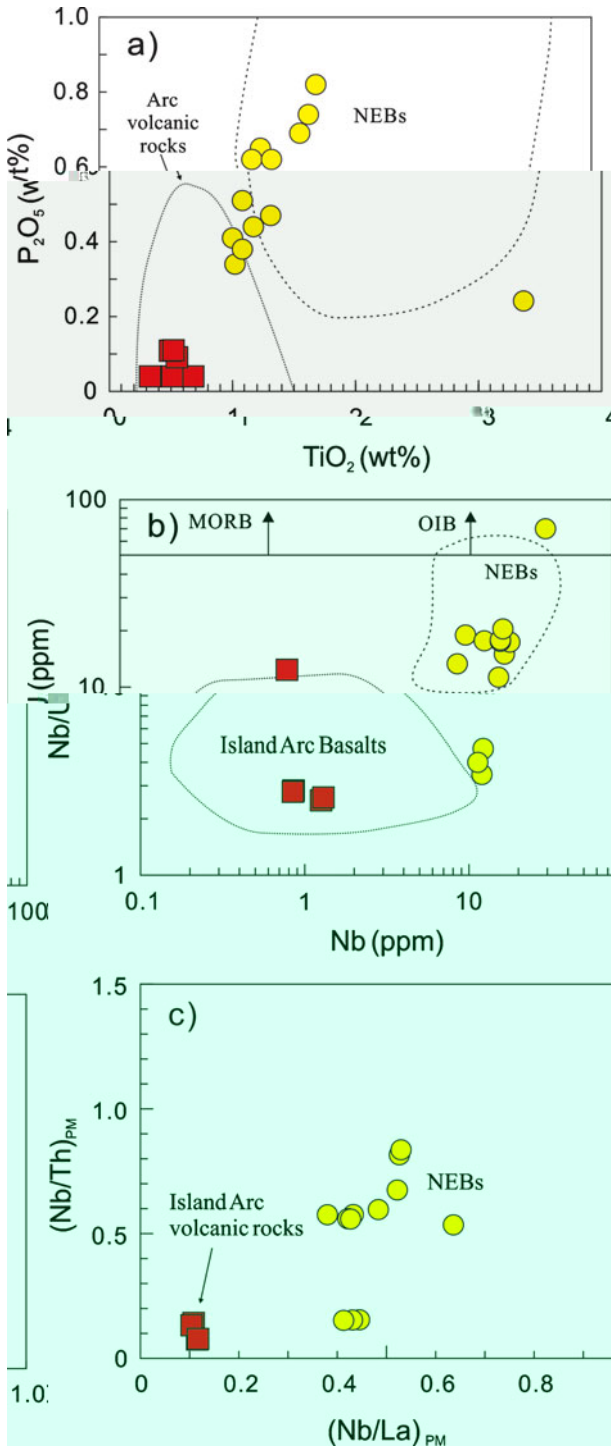


Figure 14. (a) P₂O₅ vs TiO₂ diagram showing the distribution of the Zhaheba ophiolite (red squares) and NEBs (yellow circles). (b) Nb/U vs Nb diagram showing the distribution of the Zhaheba ophiolite (red squares) and NEBs (yellow circles). (c) (Nb/Th)_{PM} vs (Nb/La)_{PM} diagram showing the distribution of the Zhaheba ophiolite (red squares) and NEBs (yellow circles). The shaded area represents the field for Island Arc Basalts. MORB = Mid-Ocean Ridge Basalt; OIB = Ocean Island Basalt; NEBs = Nainiang Basin Basalts.

400 3 5. (c) The Zhaheba ophiolite (red squares) and NEBs (yellow circles) are plotted on the (Nb/Th)_{PM} vs (Nb/La)_{PM} diagram. The shaded area represents the field for Island Arc Basalts. MORB = Mid-Ocean Ridge Basalt; OIB = Ocean Island Basalt; NEBs = Nainiang Basin Basalts.

(c) The Zhaheba ophiolite (red squares) and NEBs (yellow circles) are plotted on the (Nb/Th)_{PM} vs (Nb/La)_{PM} diagram. The shaded area represents the field for Island Arc Basalts. MORB = Mid-Ocean Ridge Basalt; OIB = Ocean Island Basalt; NEBs = Nainiang Basin Basalts.

(c) The Zhaheba ophiolite (red squares) and NEBs (yellow circles) are plotted on the (Nb/Th)_{PM} vs (Nb/La)_{PM} diagram. The shaded area represents the field for Island Arc Basalts. MORB = Mid-Ocean Ridge Basalt; OIB = Ocean Island Basalt; NEBs = Nainiang Basin Basalts.

(c) The Zhaheba ophiolite (red squares) and NEBs (yellow circles) are plotted on the (Nb/Th)_{PM} vs (Nb/La)_{PM} diagram. The shaded area represents the field for Island Arc Basalts. MORB = Mid-Ocean Ridge Basalt; OIB = Ocean Island Basalt; NEBs = Nainiang Basin Basalts.

(c) The Zhaheba ophiolite (red squares) and NEBs (yellow circles) are plotted on the (Nb/Th)_{PM} vs (Nb/La)_{PM} diagram. The shaded area represents the field for Island Arc Basalts. MORB = Mid-Ocean Ridge Basalt; OIB = Ocean Island Basalt; NEBs = Nainiang Basin Basalts.

(c) The Zhaheba ophiolite (red squares) and NEBs (yellow circles) are plotted on the (Nb/Th)_{PM} vs (Nb/La)_{PM} diagram. The shaded area represents the field for Island Arc Basalts. MORB = Mid-Ocean Ridge Basalt; OIB = Ocean Island Basalt; NEBs = Nainiang Basin Basalts.

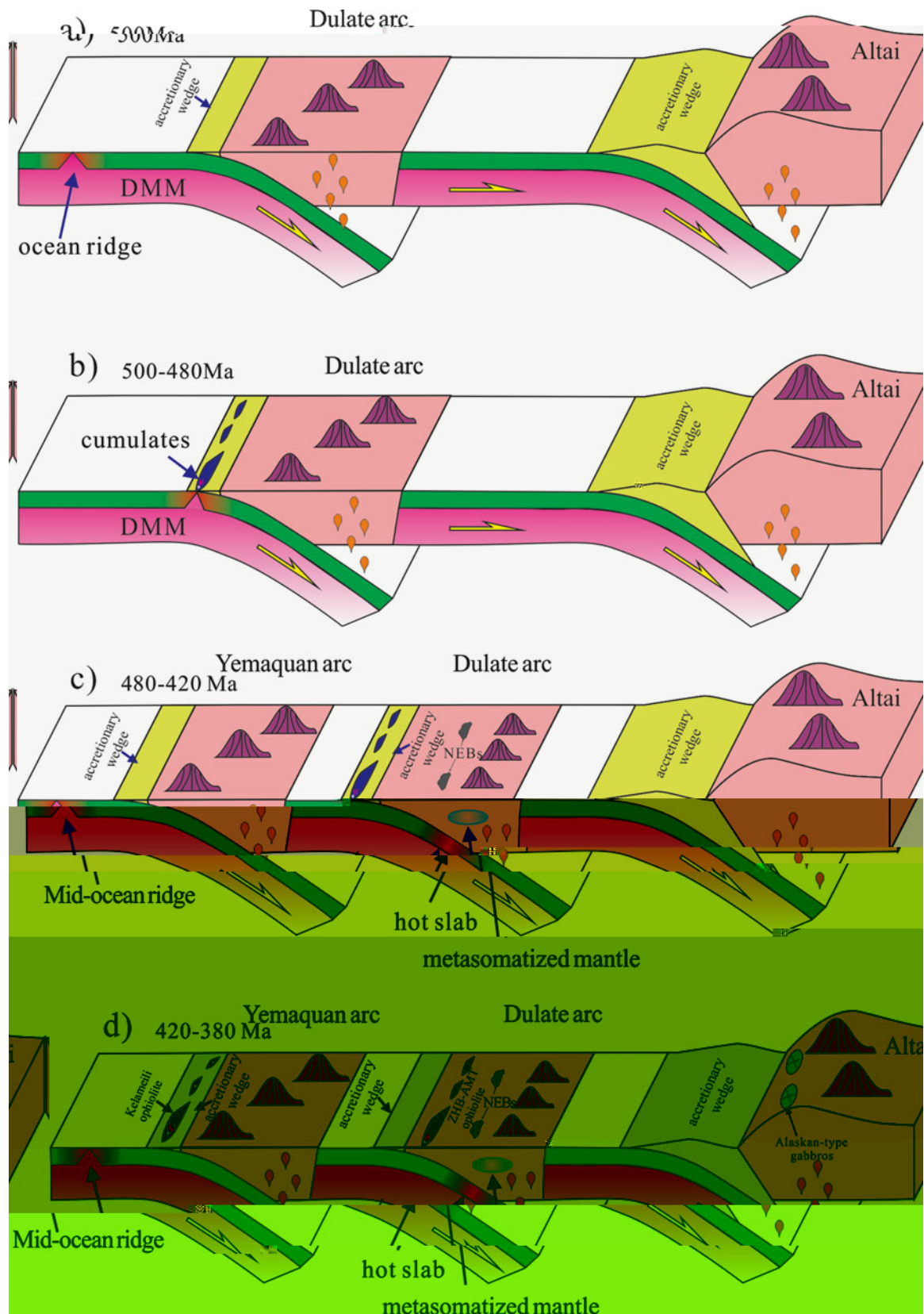


Figure 15. (a) 500 Ma, (b) 500-480 Ma, (c) 480-420 Ma, (d) 420-380 Ma. The figure shows the evolution of the Dulate and Yemaquan arcs and the Altai region over time.

- ... & ... 2011. ...
Geological Bulletin of China **30**, 150–153 (...)
 ...)
- & ... 2011. ...
Acta Geochimica et Cosmochimica **75**, 504–512.
- ... & ... 2001. ...
Nature **410**, 6–11.
- ... & ... 2002. ...
Chemical Geology **182**, 22–35.
- ... & ... 1996. ...
Journal of Geophysical Research: Solid Earth (1978–2012) **101**, 11–31.
- ... & ... 2000. ...
Contributions to Mineralogy and Petrology **139**, 20–26.
- ... & ... 2012. ...
Geological Bulletin of China **31**, 126 (...)
- ... & ... 2014. ...
Chinese Science Bulletin (Chinese Version) **59**, 2213–2221.
- ... & ... 2000. ...
Transactions of the Royal Society of Edinburgh: Earth Sciences **91**, 1–13.
- ... & ... 2010. ...
Journal of Petrology **31**, 6–11.
- ... & ... 2003. ...
Earth Science Frontier **10**, 43–56 (...)
- ... & ... 2001. ...
Journal of Petrology **42**, 655–671.
- ... & ... 2001. ...
Nature **380**, 23–40.
- ... & ... 2000. ...
Tectonophysics **326**, 255–261.
- ... & ... 2010a. ...
Lithos **114**, 1–15.
- ... & ... 2004. ...
Geological Magazine **141**, 225–231.
- ... & ... 2010b. ...
Geostandards and Geoanalytical Research **34**, 11–34.
- ... & ... 2013. ...
Chinese Science Bulletin **58**, 464–474.
- ... & ... 2000. ...
Lithos **113**, 2–4–1.
- ... & ... 2010. ...
Chinese Science Bulletin **55**, 1535–1546.
- ... 2003. *User's Manual for Isoplot 3.00: A Geochronological Toolkit for Microsoft Excel*. ...
 4, 3–11.
- ... & ... 2015. ...
Gondwana Research, 1–6 (2015).
[10.1016/j.gr.2015.04.004](https://doi.org/10.1016/j.gr.2015.04.004).
- ... & ... 2014. ...
American Journal of Science **274**, 32–355.
- ... & ... 1995. ...
Geology **23**, 51–54.
- ... 1991. *Structure of Ophiolites and Dynamics of Oceanic Lithosphere*. ...
 36–11.
- ... 1991. ...
Journal of Petrology **38**, 104–114.
- ... & ... 2000 a. ...
Acta Petrologica Sinica **25**, 16–24 (...)
- ... & ... 2000 b. ...
Acta Petrologica Sinica **25**, 14–21 (...)
- ... & ... 2000. ...
Acta Petrologica Sinica **23**, 162–174 (...)
- ... & ... 2002. ...
Proceedings of the Ocean Drilling Program, Scientific Results, vol. 176 (...)
 11, 1–60.

... & ... 200 .
 ... Chinese Science Bulletin 14, 21 6 . 1 .
 2010. ... Lithos 117, 1 20 .
 ... 200 . %
 ... Journal of Asian Earth Sciences 30, 666 5 .
 ... Lithos 100, 14 4 .
 2014. ... Elements 10, 101 .
 ... 2001. ... Contribution to Mineralogy and Petrology 141, 36 52 .
 ... 2013. ... Gondwana Research 24, 3 2 411 .
 ... Journal of Petrology 37, 6 3 26 .
 ... 2013. ... Precambrian Research 231, 301 24 .
 ... 2012. ... Precambrian Research 192–195, 1 0 20 .
 ... Philosophical Transactions of the Royal Society of London 335, 3 2 .
 ... 2015. ... Nature 377, 5 5 600 .
 ... Nature 364, 2 30 .
 2014. ... Lithos 206–207, 234 51 .
 ... 2002. ... Reviews of Geophysics 40, 3-1 3-3 .
 ... 200 . %
 ... Science in China Series D – Earth Sciences 52, 1345 5 .
 ... Magmatism in the Ocean Basin (... % , 11.52 4 .
 ... 42 .
 ... 200 .
 ... Chemical Geology 247, 352 3 .
 ... 200 . %
 ... Acta Petrologica Sinica 23, 1 33 44 (...) .
 ... Contributions to Mineralogy and Petrology 133, 1 11 .
 ... 2006. ... Journal of Geology 114, 35 51 .
 ... 200 . Lithos 110, 35 2 .
 ... 2012. ... Earth-Science Reviews 113, 303 41 .
 ... 2006. ... Chemical Geology 20, 325 43 .
 ... 2002. ... Journal of Geology 110, 1 3 .
 ... 2006. ... Geology in China 33, 4 6 6 (...) .
 ... 2014. ... Geoscience Frontiers 5, 525 36 .
 ... 200 . %
 ... Journal of Asian Earth Sciences 32, 102 1 .
 ... 2013. ... Gondwana Research 23, 1316 41 .
 ... 2004. ... Journal of Geological Society, London 161, 33 42 .

200. a. & . 2006. *Chemical Geology* **242**, 22–31.
- b. & . 2006. *Acta Geologica Sinica* **80**, 254–63 (in Chinese with English abstract).
- & . 2003. *Chinese Science Bulletin* **48**, 2231–5.
- & . 2013. *Lithos* **179**, 263–4.
- & . 2012. *Journal of Asian Earth Sciences* **52**, 11–33.
- & . 200. *Acta Petrologica Sinica* **24**, 1054–5 (in Chinese with English abstract).
- & . 196. *Annual Review of Earth and Planetary Sciences* **14**, 43–51.
200. a. & . 2006. *International Journal of Earth Sciences* **98**, 11–21.
- b. & . 2006. *American Journal of Sciences* **309**, 221–0.
1. 3. *Regional Geology of the Xinjiang Uygur Autonomous Region*. *Geological Survey of China*, 11.2 145 (in Chinese).
- & . 2015. *Journal of Asian Earth Sciences* **113**, 5.
- & . 2012. *Gondwana Research* **21**, 246–65.
- & . 200. *Acta Geologica Sinica* **80**, 254–63 (in Chinese with English abstract).